

# **Shift in the metabolic profile of sediment microbial communities during seagrass decline**

Marsej Markovski<sup>1</sup>, Mirjana Najdek<sup>1</sup>, Zihao Zhao<sup>2</sup>, Gerhard J. Herndl<sup>2,3</sup>, and Marino Korlević<sup>1\*</sup>

1. Centre for Marine Research, Ruđer Bošković Institute, Croatia
2. Department of Functional and Evolutionary Ecology, University of Vienna, Austria
3. Department of Marine Microbiology and Biogeochemistry, Royal Netherlands Institute for Sea Research (NIOZ), Utrecht University, The Netherlands

\*To whom correspondence should be addressed:

Marino Korlević

G. Paliaga 5, 52210 Rovinj, Croatia

Tel.: +385 52 804 768

e-mail: marino.korlevic@irb.hr

# <sup>1</sup> Abstract

<sup>2</sup> **Background** Seagrass meadows are highly productive ecosystems that are considered hotspots  
<sup>3</sup> for carbon sequestration and microbial activity. In seagrass sediments, microbial communities  
<sup>4</sup> break down organic matter, facilitating the release and transformation of nutrients that support plant  
<sup>5</sup> growth and primary production. The decline of seagrass meadows of various species has been  
<sup>6</sup> documented worldwide, including that of *Cymodocea nodosa* (Ucria) Ascherson, a widespread  
<sup>7</sup> seagrass in the Mediterranean Sea. To assess the influence of seagrass decline on the metabolic  
<sup>8</sup> profile of sediment microbial communities, metaproteomes from two sites, one without vegetation  
<sup>9</sup> and one with a declining *Cymodocea nodosa* meadow, were characterised at monthly intervals from  
<sup>10</sup> July 2017 to October 2018.

<sup>11</sup> **Results** Prior to seagrass decline, differences in the metabolic profiles between the vegetated  
<sup>12</sup> and nonvegetated sediment were found, particularly in the deeper sediment layers. During the  
<sup>13</sup> decline, these differences diminished as microbial communities in nonvegetated sediments exhibited  
<sup>14</sup> increased protein richness and diversity, aligning more closely with those at the vegetated site.  
<sup>15</sup> Notably, temporal variations in the structure of the metabolic profile were only observable in  
<sup>16</sup> the nonvegetated sediment and were also more pronounced at greater sediment depths. Finally,  
<sup>17</sup> the assessment of proteins involved in organic matter degradation such as ABC transporters,  
<sup>18</sup> fermentation-mediating enzymes, and proteins involved in dissimilatory sulphate reduction mirrored  
<sup>19</sup> these shifts.

<sup>20</sup> **Conclusions** Overall, the main results of this study suggest that the presence of seagrass meadows  
<sup>21</sup> influences the metabolic profile of microbial communities in sediments, highlighting the distinctions  
<sup>22</sup> between nonvegetated and seagrass-colonised sediments. In particular, the loss of seagrass leads to a  
<sup>23</sup> shift in the metabolic profile of sediment communities in the surrounding area, while the metabolic  
<sup>24</sup> profiles of previously colonised sediments appear to be more resilient to seagrass loss.

<sup>25</sup> **Keywords** sediment microbial communities, *Cymodocea nodosa*, seagrass meadow decline,  
<sup>26</sup> northern Adriatic Sea, metaproteomics, microbial metabolic profile

27 **Background**

28 The biomass in marine sediments consists mainly of prokaryotes, whose richness and  
29 abundance are comparable to that in the water column [1–3]. The main factor determining the  
30 abundance and activity of these microorganisms is the availability of organic matter [3–5]. The  
31 complete mineralisation of organic compounds in anoxic environments such as most coastal  
32 sediments requires complex microbial interactions [6–9]. The stepwise degradation of organic  
33 matter begins with the breakdown of complex organic polymers such as carbohydrates or proteins  
34 by extracellular enzymes that can be released into solution or remain associated with the cell. These  
35 enzymes convert high-molecular-weight organic matter to substrates that are small enough to be  
36 transported into the cell [10]. Part of these hydrolytic products are fermented to short-chain fatty  
37 acids (SCFAs) and alcohols that facilitate anaerobic microbial respiration, e.g. by sulphate-reducing  
38 bacteria or methanogens [7, 9].

39 Shallow coastal sediments colonised by seagrasses are considered a special type of habitat  
40 where microbes break down organic matter, facilitating the release and transformation of nutrients  
41 that support plant growth and primary production [11]. Such areas are hotspots for microbial activity,  
42 as seagrasses enrich the sediment with organic matter by excreting organic carbon, trapping organic  
43 particles from the water column, and stabilising the sediment. In addition, the decomposition of  
44 seagrass leaves, roots, and rhizomes contributes to the enrichment of the sediment with organic  
45 matter [11–14]. Consequently, microbial communities in seagrass sediments are metabolically  
46 more diverse and active than those inhabiting bare sediments [15]. Taxonomic analyses showed  
47 differences between communities at vegetated and nonvegetated sites [16–21] and indicated that  
48 microbial communities even differ with respect to the meadow edge [22].

49 In order to obtain a comprehensive overview of the microbial communities living in sediments  
50 colonised by seagrasses, methods that allow functional characterisation, such as metaproteomics,  
51 must be applied. This high-throughput “meta-omics” approach is emerging as an important tool

52 for deciphering the key components that determine the function of microbial ecosystems [23]. In  
53 addition, this approach has the potential to provide insights into the biogeochemical cycling in marine  
54 sediments and to assess the response of microbes to environmental change [24]. Metaproteomics  
55 is closely linked to metagenomics, as genome information in combination with data on expressed  
56 proteins not only provides information on the functional potential of microbial populations, but  
57 also on which metabolism is active in an ecosystem [25]. Metaproteomics has already been used to  
58 analyse microbial metabolic processes in cold seeps [26, 27], diffuse hydrothermal venting [28],  
59 mudflat aquaculture [29], and chronically petroleum-polluted [30] sediments, but to our knowledge  
60 there are no metaproteomic studies on microbial communities in seagrass meadow sediments.

61 About 19 % of seagrass meadows worldwide have been lost since 1880 [31]. A decline of  
62 *Cymodocea nodosa* (Ucria) Ascherson, a widespread and common seagrass species throughout the  
63 Mediterranean Sea [32], has been observed [33–36], including in the northern Adriatic Sea [37–39].  
64 However, there is little information on microbial dynamics during seagrass decline, making it  
65 difficult to predict how the loss of seagrass influences the microbial community in the sediment. The  
66 few available studies on microbial community succession in seagrass sediments suggest that changes  
67 could be expected. For instance, changes in sulphate-reducing bacteria in seagrass bed sediments  
68 over time were reported [40], as well as community changes in response to nutrient availability  
69 [41] and seagrass restoration [42]. However, in a previous study, we investigated the diversity and  
70 dynamics of sediment microbial communities during the decline of the seagrass species *C. nodosa*  
71 and found a notable compositional stability in response to such a major disturbance [21]. The aim  
72 of the present study was to characterise the metabolic profile of prokaryotic communities in *C.*  
73 *nodosa* meadow sediments using a metaproteomic approach, with the hypotheses that: (i) there  
74 are differences in metabolic profiles between vegetated and nonvegetated sediments that vary with  
75 sediment depth, and (ii) the decline of seagrass meadows leads to a shift in the microbial metabolic  
76 profile that is not uniform across sediment layers.

77 **Methods**

78 **Sampling**

79 Sampling for DNA and protein isolation was performed as described in Markovski et al. (2022)  
80 [21]. Briefly, sediment samples were collected in a declining *C. nodosa* meadow (vegetated site)  
81 in the Bay of Saline, a shallow and dynamic coastal area 4 km north-west of Rovinj, Croatia, on  
82 the east coast of the northern Adriatic Sea (45°7'5" N, 13°37'20" E). An adjacent area without  
83 seagrass (nonvegetated site) was also sampled in the same bay. From July 2017 to October 2018,  
84 a sediment core was taken monthly at each site by diving with plastic core samplers. As seagrass  
85 surface sediments show vertical patterns of environmental conditions [39] and microbial community  
86 structures [19], the sediment cores were cut into four sections of 1 cm length each: the top (0 – 1  
87 cm), the bottom (7 – 8 cm), and two middle sections: upper middle (2 – 3 cm) and lower middle (3  
88 – 6 cm; Supplementary Table S1). A detailed description of the sampling site, the environmental  
89 conditions, and the decline of the *C. nodosa* meadow can be found in Najdek et al. (2020) [39]. In  
90 brief, at the beginning of the study, part of the bay was covered with a large and dense seagrass  
91 meadow extending from the south-western coastal area towards the central part of the bay. The  
92 seagrass showed a regular growth minimum in November 2017. After that, the shoots and leaves  
93 began to decline, while roots and rhizomes persisted longer, until March 2018. At the end of the  
94 study, only small patches of the meadow were still present in the form of tiny strips along the  
95 shoreline [39]. The decline of the meadow was attributed to the reduced light availability caused by  
96 the increased turbidity of the seawater due to the increased terrigenous input [39].

97 **DNA isolation**

98 Total DNA from each sediment section was isolated using a modified isolation protocol [43]  
99 based on Zhou et al. (1996) [44] as described in Markovski et al. (2022) [21]. In brief, 2 g of

100 sediment were weighed, avoiding roots and rhizomes in vegetated cores, mixed with the extraction  
101 buffer and proteinase K, and incubated by horizontal shaking at 37 °C for 30 min. After the addition  
102 of SDS, the mixture was incubated again by horizontal shaking at 65 °C for 60 min. The sediment  
103 particles were removed by centrifugation and the supernatant was extracted three times with an  
104 equal volume of chloroform:isoamyl alcohol (1:1). DNA precipitation was performed by adding  
105 isopropanol and incubating the mixture at 22 °C for 60 min. The DNA pellet obtained after the  
106 centrifugation step was washed twice with cold (–20 °C) 70 % ethanol, air-dried, and resuspended  
107 in 100 µl of deionised water.

## 108 Metagenomics

109 Due to the limited number of sediment metagenomes that could have been sequenced, we  
110 selected four DNA samples from Markovski et al. (2022) [21] collected in August 2018 from  
111 the top (0 – 1 cm) and lower middle (4 – 5 cm) layers of both the vegetated and nonvegetated  
112 sites (Supplementary Table S2). These selected DNA samples were sent on dry ice to IMGM  
113 Laboratories (Martinsried, Germany) for metagenomic sequencing. The genomic DNA was purified  
114 using AMPure XP Beads (Beckman Coulter, USA) at a bead:DNA ratio of 1:1 (v/v) and quantified  
115 using the Qubit dsDNA HS Assay Kit (Thermo Fisher Scientific, USA). The integrity of the DNA  
116 was checked on a 1 % agarose gel. Metagenomic sequencing libraries were prepared from 100 or  
117 300 ng of genomic DNA using the NEBNext Ultra II FS DNA Library Prep Kit for Illumina (New  
118 England Biolabs, USA) according to the manufacturer’s protocol. Fragments of 500 – 700 bp were  
119 selected using the AMPure XP Beads, enriched by PCR for 5 or 6 cycles, and quality controlled.  
120 The individual libraries generated from different DNA input samples were pooled and sequenced on  
121 an Illumina NovaSeq 6000 sequencing system (2 × 250 bp).

122 The sequences obtained were analysed on the Life Science Compute Cluster (LiSC; CUBE  
123 – Computational Systems Biology, University of Vienna). MEGAHIT (version 1.2.9) [45], with

124 default settings, was used to assemble individual metagenomic libraries and putative genes were  
125 predicted from contigs longer than 200 bp using Prodigal (version 2.6.3) [46] in metagenome mode  
126 (-p meta). Predicted genes were functionally annotated using the eggNOG mapper (version 2.1.9)  
127 [47] with the eggNOG database (version 5.0.2) [48]. Taxonomic classification was performed  
128 using the lowest common ancestor algorithm from DIAMOND (version 2.0.15) [49] against the  
129 non-redundant NCBI database (NR). Phylogeny was determined using the top 10 % of hits with  
130 an e-value  $< 1 \times 10^{-5}$  (--top 10). Sequence renaming and the calculation of metagenomic statistics  
131 were performed using the tools from BBTools (<https://jgi.doe.gov/data-and-tools/bbtools>). In  
132 total, metagenomic sequencing generated between 205,085,833 and 216,556,629 sequence pairs  
133 (Supplementary Table S2). After the removal of low-quality reads, sequences were assembled  
134 into 21,634,340 to 33,248,196 contigs, with L50 ranging from 590 to 601 bp. Coding sequence  
135 (CDS) prediction generated between 27,526,969 and 42,249,295 CDSs, while functional annotation  
136 resulted in 19,599,377 to 29,892,039 annotated CDSs.

## 137 Protein isolation

138 The proteins were isolated from the same sediment sections that were used for DNA isolation  
139 [21]. For each of the 15 sampling dates, one protein sample was isolated for each of the four  
140 sections collected from the vegetated and nonvegetated site, resulting in a total of 120 protein  
141 samples (Supplementary Table S1). The SDS-based lysis method with trichloroacetic acid (TCA)  
142 precipitation described in Chourey et al. (2010) [50] and modified by Hultman et al. (2015) [51] was  
143 used. To 5 g of sediment, 10 % (w/w) polyvinylpolypyrolidone (PVPP) was added. The mixture  
144 was suspended in 5 ml protein extraction buffer (4 % SDS; 100 mM Tris-HCl, pH 8.0) and vortexed.  
145 After incubation in boiling water for 5 min, the samples were sonicated and incubated again in  
146 boiling water for 5 min. Sonication was performed using the Sonopuls HD 4100 probe sonicator  
147 (Bandelin, Germany) equipped with an UW 100 ultrasonic transducer and a TS 103 probe. The  
148 solution was sonicated at 75 % of the maximum amplitude (245  $\mu\text{m}$ ) for 2 min at an interval of

149 10 s on and 10 s off. The sediment particles were removed by centrifugation for 20 min at 4 °C  
150 and 4,500 × g. The supernatant was transferred to a clean tube and mixed with 1 M dithiothreitol  
151 (DTT; final concentration 24 mM). The proteins were precipitated with cold (4 °C) 100 % TCA  
152 (final concentration 20 %) overnight at –20 °C. The protein pellet was obtained by centrifugation  
153 for 40 min at 4 °C and 10,000 × g. The obtained pellet was washed three times with cold (–20 °C)  
154 acetone and centrifuged after each washing step for 5 min at 4 °C and 20,000 × g. The pellet was  
155 transferred to a clean 1.5 ml tube during the first washing step. The dried pellet was stored at –80 °C  
156 until further processing.

## 157 Metaproteomics

158 The filter-aided sample preparation (FASP) [52] procedure was used to perform trypsin  
159 digestion. Isolated proteins were processed using the FASP Protein Digestion Kit (Expedeon,  
160 UK) according to the manufacturer's instructions, with minor modifications [53]. Briefly, the  
161 protein pellet was solubilised in the urea sample buffer included in the kit, amended with DTT,  
162 and centrifuged to remove larger particles. The trypsin digestion was performed on the column  
163 filter overnight at 37 °C for 18 h. The resulting filtrate containing peptides was acidified to a final  
164 concentration of 1 % trifluoroacetic acid (TFA). Digested peptides were desalted using the Pierce  
165 C18 Tips (Thermo Fisher Scientific, USA) according to the manufacturer's instructions and sent to  
166 the Proteomics Facilities of the University of Vienna for mass spectrometry analysis.

167 MS/MS spectra were obtained using a Q Exactive Hybrid Quadrupole-Orbitrap Mass  
168 Spectrometer (Thermo Fisher Scientific, USA) and searched against a protein database containing  
169 amino acid sequences of predicted CDSs from combined metagenomes that were sequenced  
170 and analysed as described above. MS/MS spectra were successfully generated for 118 samples  
171 (Supplementary Table S1). Before the protein database search, the predicted CDSs were clustered  
172 at 90 % similarity using CD-HIT (version 4.6.8). Peptides were identified using the SEQUEST-HT

173 engine and validated with Percolator, all within Proteome Discoverer (version 2.1; Thermo Fisher  
174 Scientific, USA). The probability of false peptide identification was reduced by applying the  
175 target-decoy approach. Only peptides with a false discovery rate < 1 % were retained. Protein  
176 identification required at least two peptides, including one unique peptide. Quantification of the  
177 relative abundance of proteins was conducted using a chromatographic peak area-based label-free  
178 quantitative method [54, 55], where the peak areas of unique peptides were summed and normalised  
179 to the normalised area abundance factor (NAAF). In total, 67,947 different proteins were identified  
180 from the obtained MS/MS spectra. Of all identified proteins, 94.6 % were annotated by the  
181 eggNOG database. To focus exclusively on microbial communities, only proteins classified as  
182 *Archaea* and *Bacteria* using the NCBI database were retained. As a precautionary measure, proteins  
183 that were not taxonomically classified as *Archaea* or *Bacteria* by the eggNOG database were also  
184 removed, leaving a total of 57,305 proteins in the dataset.

## 185 Data analysis

186 Data processing and visualisation were performed using R (version 4.5.0) [56] combined  
187 with the tidyverse package (version 2.0.0) [57, 58] and several other packages [59–78]. The  
188 Shannon diversity index was calculated using the function *diversity* from the vegan package  
189 (version 2.6.10) [71]. To express the diversity index in terms of the effective number of proteins,  
190 the exponential of the Shannon diversity index was calculated [79]. Differences between the  
191 number of observed proteins, the exponential of the Shannon diversity index, and the NAAFs  
192 between sites, sediment layers, i.e. sections of sediment cores, and the period before and during  
193 the decline of the *C. nodosa* meadow were tested by applying the Mann-Whitney *U* test using  
194 the function *wilcox.test* [56]. The Bonferroni correction was applied to solve the problem  
195 of multiple comparisons using the function *p.adjust* [56]. Differences in the structure of the  
196 microbial metabolic profiles between sites, sediment layers, and the period before and during the  
197 meadow decline were tested on Bray-Curtis dissimilarities based on protein NAAFs by performing

198 the Analysis of Similarities (ANOSIM) using the function `anosim` from the vegan package and  
199 999 permutations [71]. The grouping of samples into the period before and during meadow decline  
200 was based on the status assessment of the *C. nodosa* meadow reported by Najdek et al. (2020)  
201 [39], focusing on the belowground biomass. The sampling period from the beginning of the study  
202 until February 2018 was labelled the period before decline, while the period after this month was  
203 referred to as the period of meadow decline. Principal Coordinate Analysis (PCoA) was performed  
204 on Bray-Curtis dissimilarities based on protein NAAFs using the function `wcmdscale` from the  
205 vegan package. If necessary, the Lingoes correction method was applied to account for negative  
206 eigenvalues [71, 80, 81].

207 **Results**

208 To assess the richness and diversity of isolated proteins from the sediment microbial  
209 communities in the Bay of Saline, the number of observed proteins and the exponential of the  
210 Shannon diversity index were calculated. Samples from each layer were grouped based on the  
211 sampling site and the period before and during the meadow decline. Comparisons were made both  
212 between sampling sites within each period and between different periods at each individual site  
213 (Fig. 1). In all layers, significantly ( $p < 0.05$ ) higher numbers of observed proteins were found  
214 during the period before meadow decline at the vegetated (top, 35,626 – 37,937 proteins; upper  
215 middle, 32,494 – 39,996 proteins; lower middle, 35,220 – 39,713 proteins; and bottom, 32,183  
216 – 37,440 proteins) compared to the nonvegetated (top, 29,217 – 36,284 proteins; upper middle,  
217 29,312 – 36,755 proteins; lower middle, 25,752 – 33,630 proteins; and bottom, 27,672 – 33,922  
218 proteins) site. In contrast, no significant changes between sites were observed in all layers during  
219 the period of decline. In addition, no significant changes were found at each site between the two  
220 periods. When analysing the exponential of the Shannon diversity index, significant changes were  
221 observed only in the lower middle and bottom layer (Fig. 1). Here, in agreement with the number  
222 of observed proteins, higher values were found during the period before meadow decline at the  
223 vegetated (lower middle 7,594.2 – 11,300.0 proteins and bottom, 3,927.3 – 10,300.9 proteins)  
224 compared to the nonvegetated site (lower middle 1,497.2 – 3,070.7 proteins and bottom, 586.6 –  
225 2,696.5 proteins). Also, in agreement with the number of observed proteins, no significant changes  
226 were observed between the sites during meadow decline. Additionally, the Shannon diversity index  
227 showed significant changes in these layers between the two periods. In the lower middle layer of  
228 the vegetated site, significantly higher values were observed before (7,594.2 – 11,300.0 proteins)  
229 than during (4,254.3 – 9,227.5 proteins) meadow decline. However, in the bottom layer of the  
230 nonvegetated site significantly higher values were found during (1,815.8 – 6,775.9 proteins) than  
231 before the meadow decline (586.6 – 2,696.5 proteins).

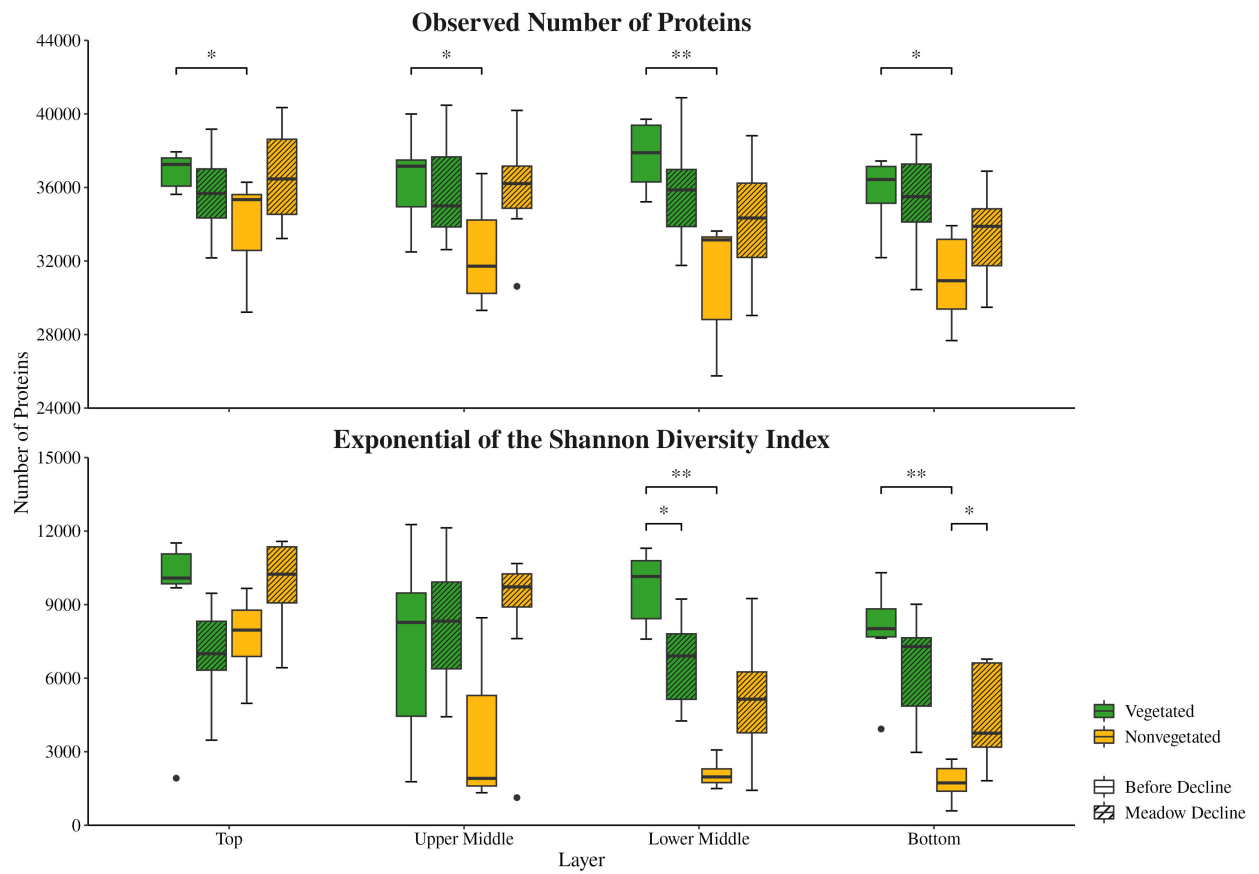


**Fig. 1** The observed number of proteins and the exponential of the Shannon diversity index of sediment microbial communities in the Bay of Saline. Samples were collected in different sediment layers at the vegetated and nonvegetated site before and during the decline of the *C. nodosa* meadow. The asterisks indicate the level of statistical significance: \* $p < 0.05$  and \*\* $p < 0.01$ , while the dots represent outliers.

ANOSIM testing of Bray-Curtis dissimilarities was applied to determine the changes in the structure of the metabolic profile of the sediment microbial communities. When all proteins from all samples were analysed together, no strong differentiation was observed between sites, layers, or the period before and during meadow decline (ANOSIM,  $R = 0.14 - 0.24$ , all  $p < 0.01$ ). To determine whether only a part of the metabolic network showed any differentiation, proteins classified in the Cluster of Orthologous Genes (COG) category C (energy production and conversion), the most abundant category in our samples (see below, Supplementary Table S3), were analysed separately. However, no strong differentiation was observed between sites, layers, or decline periods when

only these proteins were considered (ANOSIM,  $R = 0.15 - 0.21$ , all  $p < 0.01$ ). In addition, the separate analysis of samples from the vegetated and nonvegetated site of all and COG C categorised proteins did also not reveal a strong differentiation between layers or decline periods (ANOSIM,  $R = 0.09 - 0.26$ , all  $p < 0.01$ ), with the exception of a more pronounced separation observed at the nonvegetated site between the periods before and during meadow decline. This separation could be observed when all proteins (ANOSIM,  $R = 0.33, p < 0.01$ ) and, especially, when proteins from the functional COG category C (ANOSIM,  $R = 0.51, p < 0.01$ ) were considered. To gain a clearer overview of this separation, samples from the nonvegetated site were analysed using PCoA (Fig. 2). A distinction of samples from the lower middle and bottom layer retrieved during the period before meadow decline from all other samples was noticed. This distinction could be observed when all proteins were analysed together, but especially when proteins from the functional COG category C were considered (Fig. 2). Furthermore, to gain a better insight in the change of the structure of the metabolic profile between the period before and during meadow decline, samples from each site and layer were analysed separately. Sediment layers of the vegetated site did not show any strong differentiation between these two periods when either all (ANOSIM,  $R = 0.05 - 0.31, p = 0.01 - 0.24$ ) or only COG C categorised proteins (ANOSIM,  $R = 0.12 - 0.30, p = 0.01 - 0.07$ ) were considered. In contrast, a pronounced separation between the two periods was observed in different layers of the nonvegetated site (Fig. 3). When comparing the layers of this site, the lowest distinction between the two periods was observed in the top layer (ANOSIM; all proteins,  $R = 0.35, p < 0.01$ ; COG C proteins,  $R = 0.38, p < 0.01$ ), middle in the upper and lower middle layer (ANOSIM; all proteins,  $R = 0.29 - 0.45$ , all  $p < 0.01$ ; COG C proteins,  $R = 0.53 - 0.62$ , all  $p < 0.01$ ), and the highest in the bottom layer (ANOSIM; all proteins,  $R = 0.53, p < 0.01$ ; COG C proteins,  $R = 0.95, p < 0.01$ ).

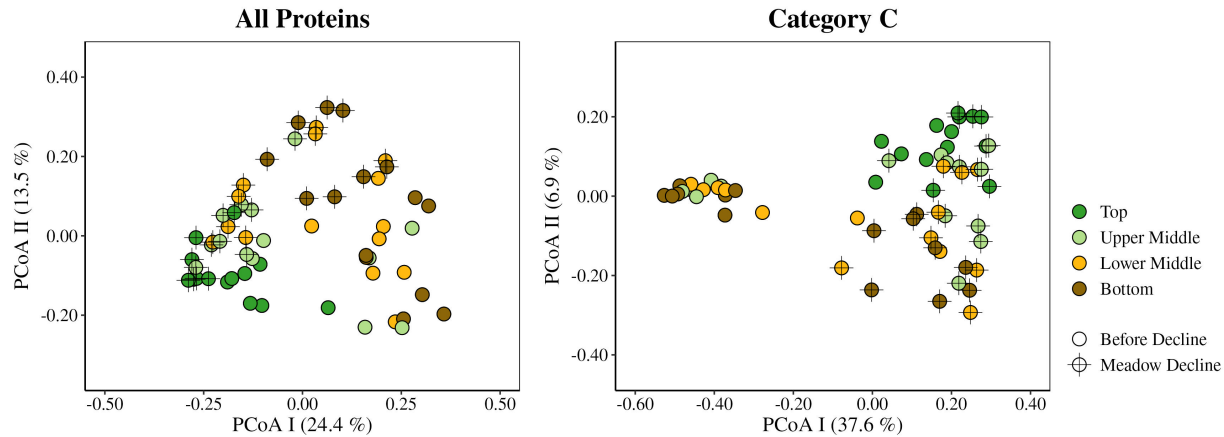


**Fig. 2** PCoA of Bray-Curtis dissimilarities of microbial proteins sampled in the sediment of the Bay of Saline. All proteins and proteins classified only into COG category C (energy production and conversion) were analysed. Only samples collected in sediment layers at the nonvegetated site before and during the decline of the *C. nodosa* meadow are shown. The proportion of variation explained by each axis is indicated in parentheses on the corresponding axis.

263 A total of 52,270 different proteins were assigned to a COG functional category. The most  
 264 abundant COG category in terms of the number of proteins it contained (8,224 proteins) and  
 265 their NAAFs (15.2 %) was the functional COG category C, which comprises proteins for energy  
 266 production and conversion (Supplementary Table S3). To detect how the decline of the meadow  
 267 affected the energy production and conversion of sediment microbial communities in the Bay of  
 268 Saline, we assessed the NAAF dynamics of the functional COG category C in each sediment  
 269 layer. When comparing the sites before the meadow decline, significant ( $p < 0.05$ ) differences  
 270 were only observed in the bottom layer where the proteins of this functional category comprised  
 271 a larger proportion at the nonvegetated (19.5 – 31.7 %) than at the vegetated (13.8 – 26.2 %) site.  
 272 No significant difference was found between the sites during the decline. When comparing the  
 273 layers of the individual sites before and during the decline, we detected a significant change in the  
 274 proportion of the functional COG category C only in the bottom layer of the nonvegetated site.  
 275 Here, a significant decrease in the proportion of this functional category was observed between the  
 276 period before (19.5 – 31.7 %) and during (8.2 – 13.9 %) meadow decline.

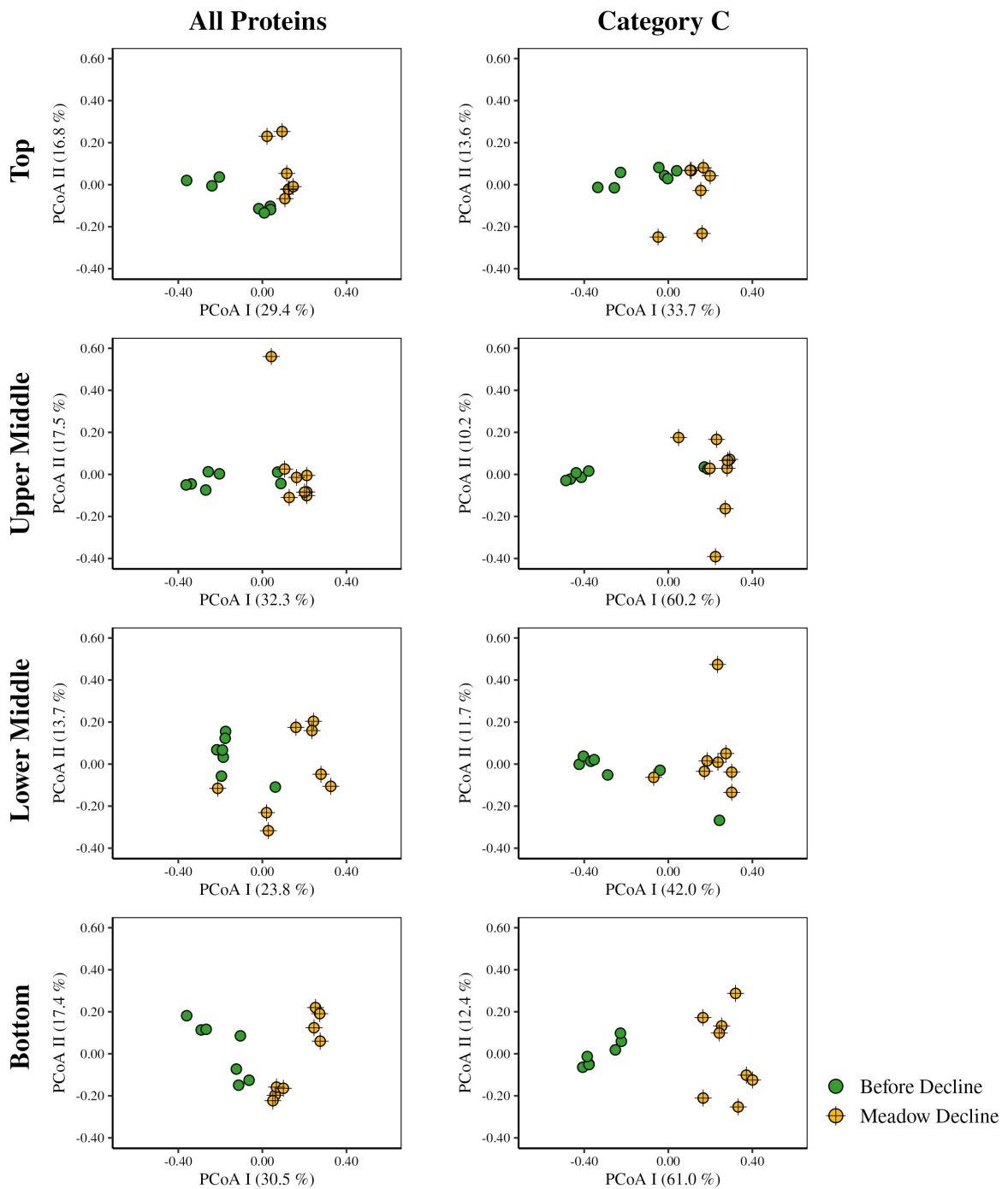


**Fig. 3** PCoA of Bray-Curtis dissimilarities of microbial proteins sampled in each layer in the sediment of the Bay of Saline. All proteins and proteins classified only into COG category C (energy production and conversion) were analysed. Only samples collected at the nonvegetated site before and during the decline of the *C. nodosa* meadow are shown. The proportion of variation explained by each axis is indicated in parentheses on the corresponding axis.

As the COG categories provide only a broad overview, the predicted CDSs were also classified using the Kyoto Encyclopaedia of Genes and Genomes (KEGG) Orthology (KO) database to gain better insight into the metabolic profile. A total of 1,408 different KO entries were present in the dataset, while 37,243 proteins were assigned to one or more of these KO entries. As the functional COG category C was the most abundant in our dataset (Supplementary Table S3), we aimed to further explore the dynamics of the most pronounced KO entries within this category. The F-type H<sup>+</sup>-transporting ATPase subunit c (ATPF0C, atpE; 20.0 %), the K<sup>+</sup>-stimulated pyrophosphate-energised sodium pump (hppA; 7.9 %), and the adenylylsulphate reductase subunits A (aprA; 6.2 %) and B (aprB; 6.1 %) represented the highest proportion (NAAF) within the functional COG category C (Fig. 4). As the samples from the nonvegetated site showed a clear separation based on the decline periods, especially when the COG category C dataset was considered (Fig. 2), we compared the proportion of these three proteins at the nonvegetated site before and during meadow decline (Fig. 4). We observed a significant ( $p < 0.05$ ) decrease in the proportion of the F-type H<sup>+</sup>-transporting ATPase subunit c during the decline in all layers. This decrease was particularly pronounced in the bottom layer, where this protein constituted between 52.7 and 76.0 % of all COG C categorised proteins before the decline. During meadow decline, its proportion dropped to between 3.2 and 19.3 %. Although not as pronounced as the change in the F-type H<sup>+</sup>-transporting ATPase subunit c, the K<sup>+</sup>-stimulated pyrophosphate-energised sodium pump also showed a significant shift between the two periods in all layers, except the top layer. The most significant shift was observed in the bottom layer, where this protein increased from between 0.8 and 4.9 % of all COG categorised proteins before the decline to between 4.9 and 11.6 % during meadow decline ( $p < 0.001$ ). The proportion of the adenylylsulphate reductase subunits A and B also increased during the decline in all layers, with the exception of the top layer. However, this shift was only significant in the bottom layer, where this protein increased from 3.5 to 7.4 % of all COG categorised proteins before the decline to 12.1 to 15.7 % during meadow decline.

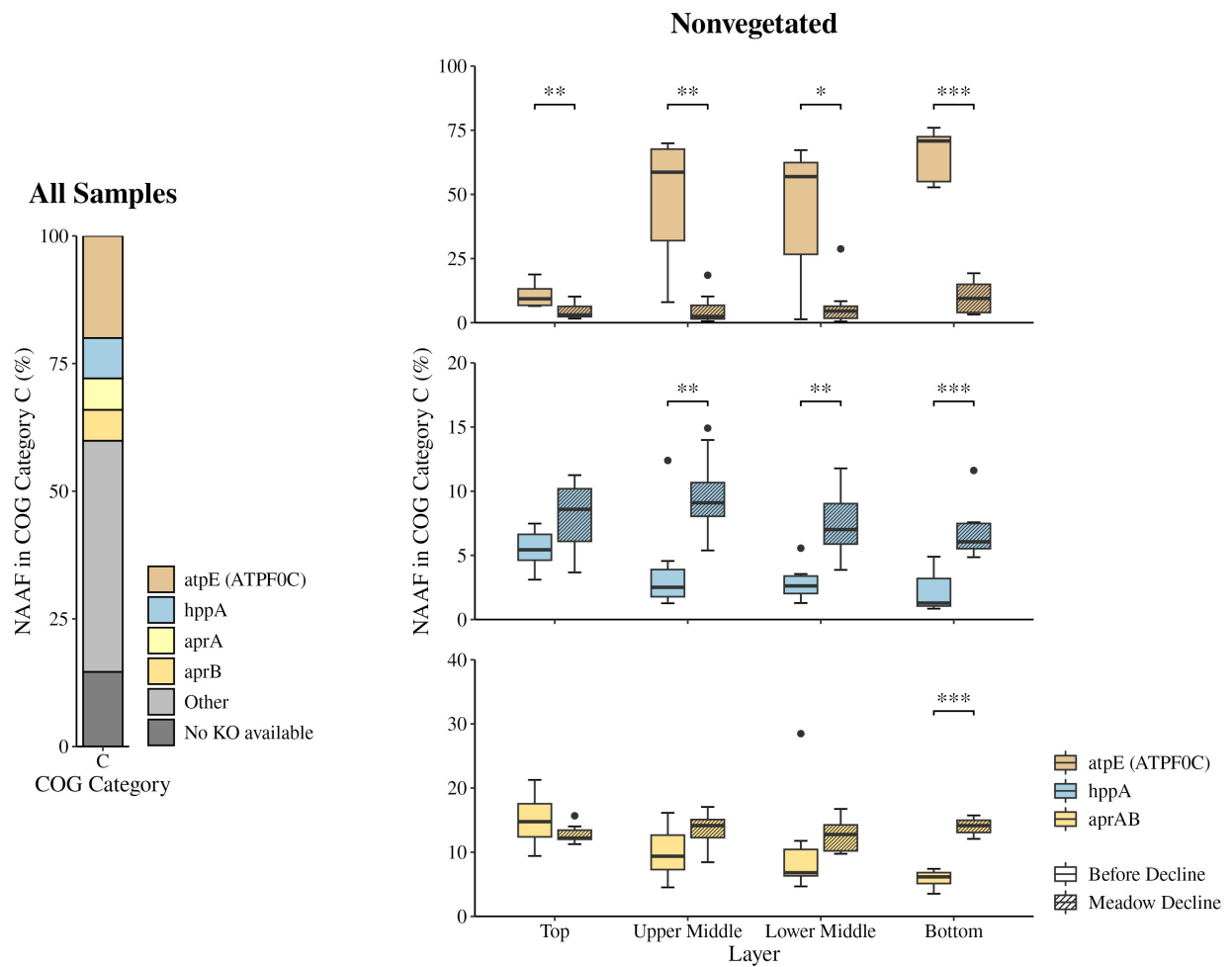


**Fig. 4** Proportion of the most abundant ( $> 3\%$ ) KEGG KO entries within the functional COG category C (energy production and conversion) in all samples and changes in the proportion of the same entries in each layer at the nonvegetated site before and during the decline of the *C. nodosa* meadow in the Bay of Saline. The proportion was calculated using the NAAF. The asterisks indicate the level of statistical significance:  $*p < 0.05$ ,  $**p < 0.01$ , and  $***p < 0.001$ , while the dots represent outliers.

The degradation of complex organic matter by the sediment microbial community in the Bay of Saline was evaluated by assessing the dynamics of the carbohydrate, protein, and lipid hydrolytic enzymes (Fig. 5). The dynamics of carbohydrate hydrolytic enzymes was determined using Carbohydrate-Active enZymes (CAZymes), whose proportion did not significantly ( $p < 0.05$ ) change between sites or decline periods, with the exception of the top sediment layer at the nonvegetated site. Here, a significant decrease in the proportion of CAZymes was observed from

308 the period before decline (0.28 – 0.43 %) to the period of meadow decline (0.22 – 0.28 %; Fig. 5).  
309 Proteins assigned to the glycoside hydrolase families GH5 and GH9 were the most abundant of all  
310 CAZymes (47.2 %). To assess protein degradation, we focused on proteins assigned as peptidases  
311 in KEGG. The proportion of these enzymes significantly increased in the upper middle layer of  
312 the vegetated site from the period before decline (0.15 – 0.45 %) to the period of meadow decline  
313 (0.34 – 0.61 %; Fig. 5). Peptidases were almost exclusively comprised of metalloendopeptidases  
314 and serine endopeptidases (93.3 %). Compared to CAZymes and peptidases, lipases were the least  
315 represented in our data (Fig. 5).

316 We assessed the dynamics of ATP-binding cassette (ABC) transporters to evaluate the uptake of  
317 hydrolytic products by prokaryotic cells. Substrate-binding proteins classified as ABC transporters  
318 in the KEGG Pathway (map02010) were selected and further manually classified into the following  
319 categories based on the molecules they transport: sugar, peptide, amino acid, urea, lipid, polyol,  
320 phosphate, and mineral and organic ion (Fig. 5). Sugar (38.0 %) and amino acid (31.5 %)  
321 transporters were the most abundant among all selected ABC transporters. In the lower middle and  
322 bottom layer, a significantly ( $p < 0.05$ ) higher proportion of sugar ABC transporters was observed at  
323 the vegetated (lower middle, 2.90 – 4.57 %; bottom, 3.90 – 5.52 %) than at the nonvegetated (lower  
324 middle, 2.25 – 3.20 %; bottom, 1.75 – 2.81 %) site during the period before meadow decline (Fig.  
325 5). In contrast, no significant differences in the proportion of ABC transporters targeting sugars  
326 between sites were observed during the period of meadow decline. These transporters also showed a  
327 significant increase in the bottom layer of the nonvegetated site from the period before decline (1.75  
328 – 2.81 %) to the period of meadow decline (2.16 – 6.79 %). The proportion of ABC transporters  
329 targeting amino acids only showed a significant increase in the bottom layer of the nonvegetated site  
330 from the period before decline (2.05 – 3.02 %) to the period of meadow decline (2.76 – 4.62 %).

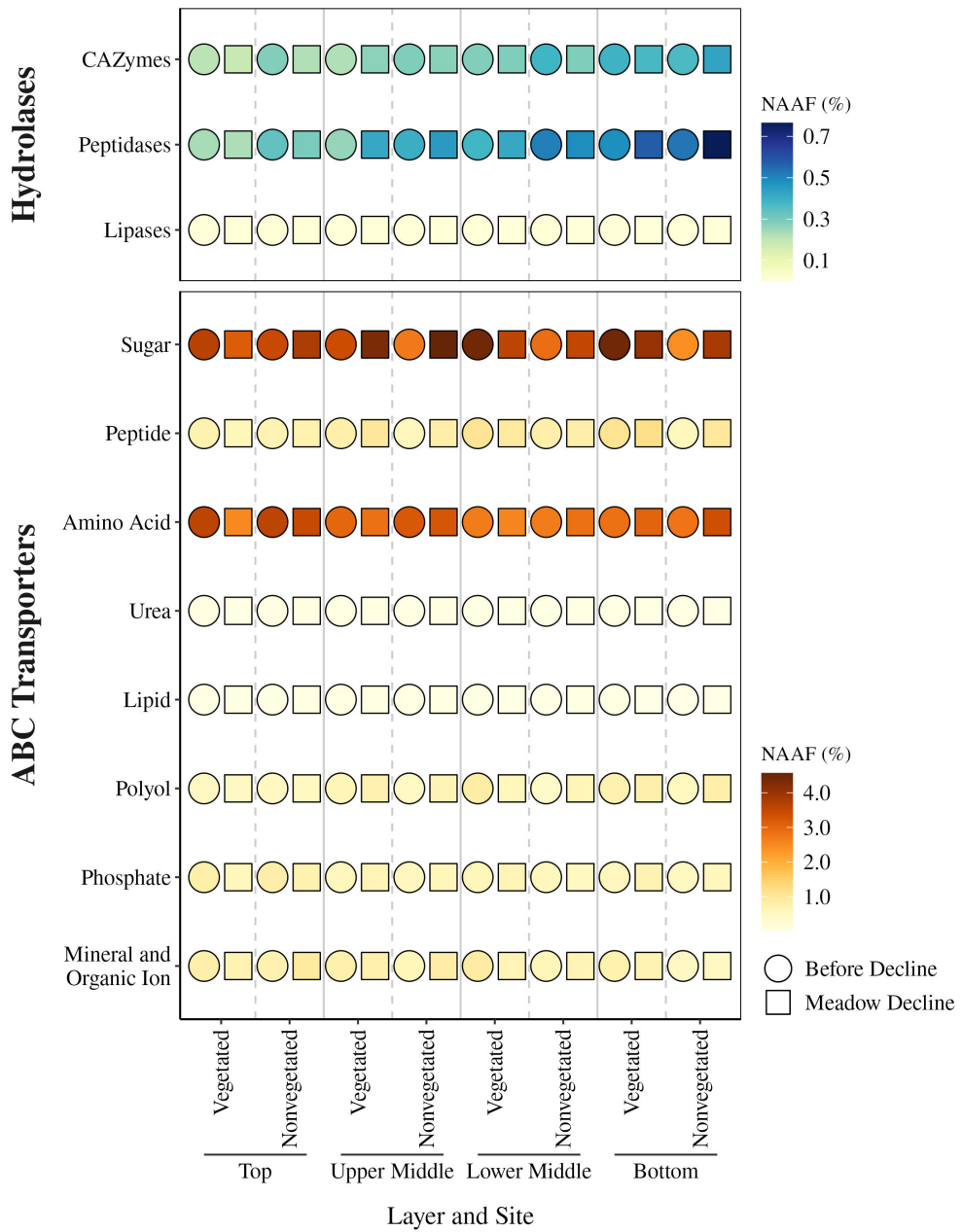


**Fig. 5** Median proportion of groups of hydrolases and ABC transporters in sediment layers at the vegetated and nonvegetated site before and during the decline of the *C. nodosa* meadow in the Bay of Saline. The proportion was calculated using the NAAF.

To evaluate the role of fermentation processes at these two sites, we selected enzymes from the KEGG database that are thought to be involved in mediating various fermentation products such as carbon dioxide, formate, acetate, acetone, ethanol, lactate, acetooin, propionate, and butyrate

334 (Supplementary Table S4). Of these selected enzymes, our dataset contained pyruvate:ferredoxin  
335 oxidoreductase, pyruvate formate-lyase, acetyl-CoA hydrolase, acetate kinase, and alcohol, formate,  
336 and lactate dehydrogenase (Fig. 6). Formate dehydrogenase (45.2 %), pyruvate:ferredoxin  
337 oxidoreductase (31.4 %), and alcohol dehydrogenase (17.0 %) were the most prominent of all  
338 fermentation-mediating enzymes detected. Significantly ( $p < 0.05$ ) higher proportions of formate  
339 dehydrogenase were detected before meadow decline in the lower middle layer of the vegetated  
340 (0.28 – 0.45 %) compared to the nonvegetated (0.20 – 0.30 %) site. In contrast, no significant  
341 differences were observed during the decline. A similar trend was observed for pyruvate:ferredoxin  
342 oxidoreductase in the bottom layer, which had a higher proportion of this enzyme before the decline  
343 at the vegetated (0.14 – 0.30 %) compared to the nonvegetated (0.09 – 0.22 %) site. However,  
344 no significant differences between sites were observed during the decline (Fig. 6). Alcohol  
345 dehydrogenase showed significant differences between sites in both the lower middle and bottom  
346 layer. In the lower middle layer, a higher proportion of this enzyme was observed at the vegetated  
347 than at the nonvegetated site before (vegetated, 0.08 – 0.16 %; nonvegetated; 0.04 – 0.07 %)  
348 and during meadow decline (vegetated, 0.07 – 0.43 %; nonvegetated; 0.04 – 0.11 %). The same  
349 pattern of higher proportions of this enzyme at the vegetated site before (vegetated, 0.08 – 0.26 %;  
350 nonvegetated; 0.05 – 0.07 %) and during meadow decline (vegetated, 0.13 – 0.88 %; nonvegetated;  
351 0.06 – 0.14 %) was also detected in the bottom layer.

352 To obtain an overview of the different microbial metabolic processes occurring in the sediment  
353 of the Bay of Saline, we selected KEGG modules describing methane-, nitrogen-, and sulphur-related  
354 processes (Supplementary Table S5). Among all tested modules we found proteins involved  
355 in the following processes: methanogenesis, nitrogen fixation, dissimilatory nitrate reduction,  
356 denitrification, assimilatory and dissimilatory sulphate reduction, and thiosulphate oxidation by  
357 the SOX complex. Since one of the most prominent proteins in the functional COG category C  
358 (energy production and conversion) was the adenylylsulphate reductase (Fig. 4), which is involved  
359 in dissimilatory sulphate reduction, the dynamics of the enzymes involved in this process were  
360 investigated in more detail (Supplementary Table S6). Of the enzymes involved in dissimilatory

sulphate reduction, our dataset contained sulphate adenylyltransferase, adenylylsulphate reductase, and dissimilatory sulphite reductase (Fig. 6). The proportion of adenylylsulphate reductase was much higher (75.0 %) than that of sulphate adenylyltransferase (11.1 %) and dissimilatory sulphite reductase (13.9 %). Significantly ( $p < 0.05$ ) higher proportions of sulphate adenylyltransferase were observed before meadow decline at the vegetated than at the nonvegetated site in the upper middle (vegetated, 0.18 – 0.55 %; nonvegetated, 0.10 – 0.28 %), lower middle (vegetated, 0.27 – 0.61 %; nonvegetated, 0.06 – 0.19 %), and bottom (vegetated, 0.17 – 0.32 %; nonvegetated, 0.06 – 0.20 %) layer. In addition, significantly higher proportions were also found in the bottom layer of the nonvegetated site during decline (0.14 – 0.35 %) compared to the period before meadow decline (0.06 – 0.20 %). Proportions of the adenylylsulphate reductase showed significant changes in the lower middle layer, where higher values were observed before meadow decline at the vegetated (1.99 – 3.05 %) compared to the nonvegetated (1.22 – 2.53 %) site. Also, in the same layer of the vegetated site significantly higher proportions were detected before decline (1.99 – 3.05 %) compared to the period of meadow decline (1.33 – 2.40 %). In the lower middle and bottom layer, dissimilatory sulphite reductase showed higher proportions before meadow decline at the vegetated (lower middle, 0.37 – 0.78 %; bottom, 0.25 – 0.42 %) than at the novegetated (lower middle, 0.16 – 0.40 %; bottom, 0.11 – 0.21 %) site. In addition, significantly higher proportions were detected in the bottom layer of the nonvegetated site during decline (0.17 – 0.39 %) compared to the period before meadow decline (0.11 – 0.21 %). In contrast, no significant differences between sites were observed during the meadow decline for either of these enzymes (Fig. 6).

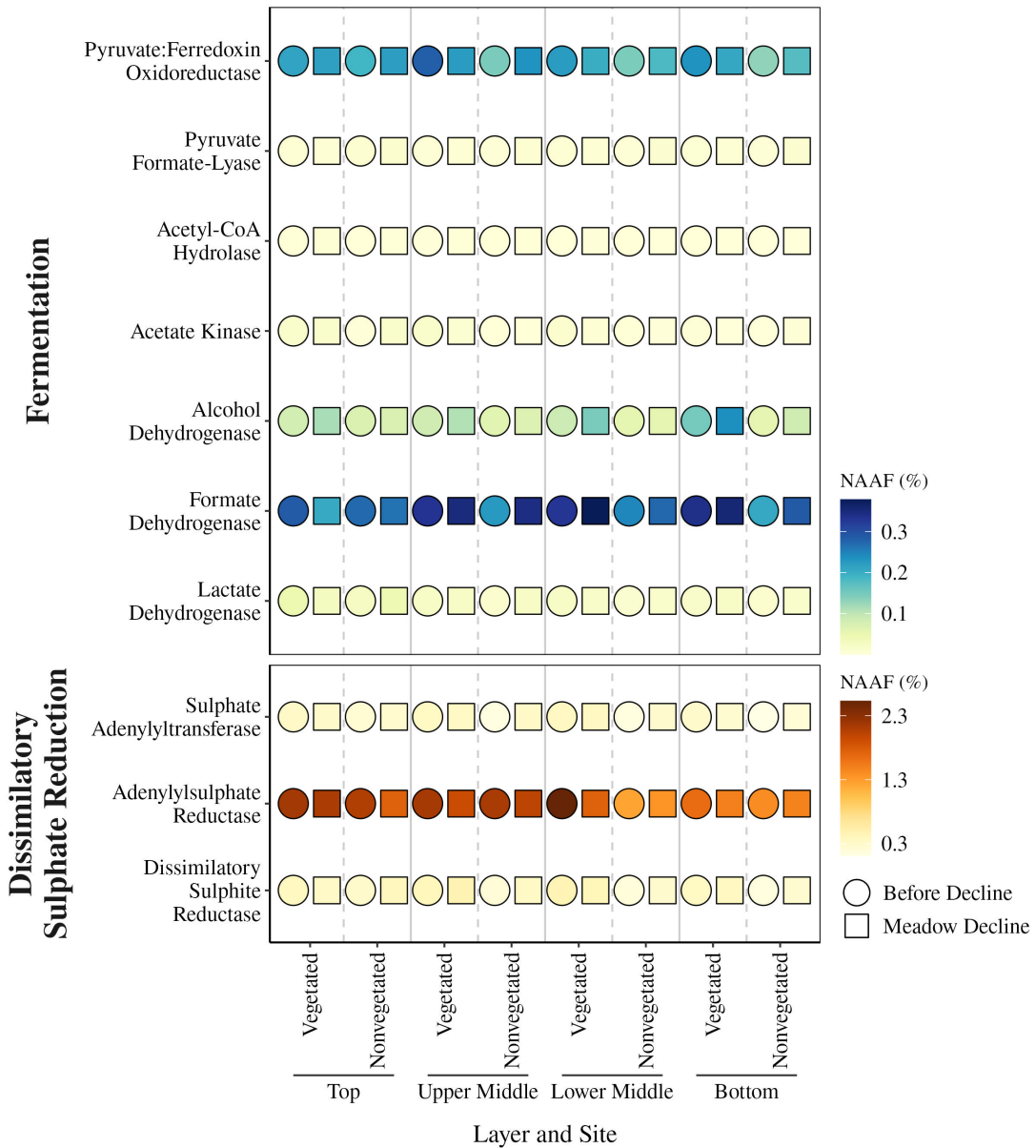


**Fig. 6** Median proportion of enzymes involved in mediating various fermentation products and dissimilatory sulphate reduction in sediment layers at the vegetated and nonvegetated site before and during the decline of the *C. nodosa* meadow in the Bay of Saline. The proportion was calculated using the NAAF.

381 **Discussion**

382 Seagrass meadow habitats are highly productive ecosystems [82] that support high biodiversity  
383 [83]. In the present study, before the decline of the *C. nodosa* meadow, higher values of the number  
384 of observed proteins and of the exponential of the Shannon diversity index were found in the  
385 vegetated compared to the nonvegetated sediment. These differences were more pronounced in the  
386 deeper parts of the sediment (i.e. in the lower middle and bottom layer). During meadow decline, the  
387 differences began to disappear and the values of the number of observed proteins and of the Shannon  
388 diversity index were similar to those observed in the sediment previously inhabited by the meadow.  
389 In addition, the structure of the metabolic profile of the communities inhabiting the nonvegetated  
390 sediment showed a separation between the period before and during meadow decline, especially in  
391 the deeper parts of the sediment and when only proteins for energy production and conversion were  
392 considered. This pattern was not observed for the communities at the vegetated site. The difference  
393 between the microbial communities inhabiting the vegetated and nonvegetated sediment in the  
394 period before meadow decline is not surprising, as several studies have found that the presence of  
395 seagrass leads to the formation of sediment communities that differ in composition [16–22] and  
396 function [15] from communities inhabiting nonvegetated sediments. In addition, the higher values  
397 of the number of observed proteins and of the Shannon diversity index at the vegetated site before  
398 the decline are consistent with other studies reporting higher metabolic diversity and microbial  
399 community activity in seagrass sediments compared to nonvegetated areas and with higher organic  
400 matter content in seagrass-inhabited sediments [11, 15]. In addition, the greater differentiation  
401 observed in the deeper layers in terms of protein richness and diversity is consistent with a previous  
402 study on the same sediment communities, which found a greater community separation between  
403 sites in the deeper parts of the sediment [21]. In contrast, the less pronounced differentiation  
404 observed for the same parameters and for the structure of the metabolic profile in the top and upper  
405 middle layer could be explained by the input of organic matter derived from the vegetated site,  
406 making the communities in the upper part of the sediment more similar to each other. Indeed,

407 organic matter imported from the seagrass meadow has been shown to be an important source for  
408 prokaryotes in nonvegetated sediments [84].

409 The lack of differences between sites during the meadow decline in the number of observed  
410 proteins and in the exponential of the Shannon diversity index indicates the presence of a more  
411 uniform microbial metabolic profile during this period, similar to the metabolic profile observed  
412 at the vegetated site prior to decline. This observation is supported by the greater similarity in the  
413 structure of the metabolic profile of the communities at the nonvegetated site during decline with  
414 the metabolic profile of the communities in the upper sediment prior to decline. Because seagrass  
415 meadows fix the sediment by reducing resuspension rates and sediment mixing [85], we hypothesise  
416 that resuspension, mixing, and transport between sites are enhanced when the meadow is no longer  
417 present, allowing greater input of fresh organic matter to the nonvegetated sediment. Indeed, Najdek  
418 et al. (2020) [39] reported higher levels of total lipids and organic matter at the nonvegetated site  
419 during the *C. nodosa* decline from May to August 2018. The uniformity of the microbial profile  
420 observed at the vegetated site during the study could be the result of maintaining the source of  
421 organic matter during the decline of the seagrass through the decay of leaves, roots, and rhizomes  
422 [11–14].

423 The analysis of the functional COG categories showed that category C, which includes  
424 proteins for energy production and conversion, was the most abundant. This is consistent with the  
425 metagenomic study of Habibi et al. (2023) [86], who reported that energy production and conversion  
426 was also one of the most abundant functional COG categories in coastal sediments. Among these  
427 proteins, F-type H<sup>+</sup>-transporting ATPase subunit c, K<sup>+</sup>-stimulated pyrophosphate-energised sodium  
428 pump, and adenylylsulphate reductase subunits A and B exhibited the highest proportion. The  
429 pronounced presence of the F-type H<sup>+</sup>-transporting ATPase subunit c in the deeper parts of the  
430 nonvegetated sediment prior to decline could be explained by the involvement of this enzyme in  
431 the generation of membrane potential. The F-type ATPase can work in both directions, utilising  
432 the proton gradient to generate ATP or hydrolysing the ATP to generate the membrane potential

[87]. The high proportion of the K<sup>+</sup>-stimulated pyrophosphate-energised sodium pump in our dataset indicates the coupling of the energy released by pyrophosphate hydrolysis with the active transport of cations across membranes [88, 89]. The proportion of this protein was increased in the deeper parts of the nonvegetated sediment during meadow decline, reflecting the need of microbial communities for more active cross-membrane transport probably due to the increased input of fresh organic matter from the vegetated site. The high proportion of adenylylsulphate reductase subunits A and B among the proteins for energy production and conversion is not surprising, as this enzyme is part of dissimilatory sulphate reduction to sulphide, a predominant terminal pathway of organic matter mineralisation in anoxic seabeds, where it reduces adenosine-5'-phosphosulphate to sulphite [90]. Furthermore, its significantly higher proportion in the nonvegetated sediment during decline could also be explained by the enhancement of this terminal pathway as a result of increased input of fresh organic matter from the vegetated site.

High molecular weight organic matter in marine sediments must be converted into low molecular weight molecules by various hydrolytic enzymes so that it can be taken up by cells [10]. Important components of organic matter in coastal marine sediments are carbohydrates, proteins, and lipids [91]. In our dataset, CAZymes and peptidases were more abundant than lipases, which may indicate the importance of carbohydrates and proteins as sources of organic matter for the microbial community. Among the CAZymes, the glycoside hydrolase families GH5 and GH9 were the most abundant. These families contain members capable of hydrolysing plant organic matter such as cellulose [92–94]. The presence of enzymes acting on cellulose is not surprising as cellulose is a major component of seagrass cell walls and contributes between 20 and 77 % to the dry plant material [95–97]. Metalloendopeptidases and serine endopeptidases made up the vast majority of peptidases in our dataset. A high proportion of these enzymes among the extracellular proteases has already been reported for coastal sediments [98–100]. CAZymes and peptidases showed no dynamics from pre-decline to meadow decline, except that CAZymes decreased in the top layer of the nonvegetated sediment and peptidases increased in the upper middle layer of the vegetated sediment. Studies have shown that the molar carbon:nitrogen content in seagrass litter decreases

460 during the decomposition process, which could be explained by increased microbial colonisation  
461 of detrital matter and microbial utilisation of exogenous nitrogen which could be related to the  
462 observed decrease in CAZymes and increase in peptidases [12, 14].

463 Once complex organic compounds have been broken down, the hydrolytic products can be  
464 transported into the cells. Prokaryotes utilise various transport proteins, including ABC transporters,  
465 to import substrates. Our metaproteomic dataset contained a large amount of ABC transporters for  
466 sugars and amino acids. Previous studies of sediment metagenomes also reported a high proportion  
467 of ABC transporters [86, 101]. The dynamics of ABC transporters reflected the overall dynamics  
468 of the metabolic profile. ABC transporters for sugars showed a higher proportion in the deeper  
469 parts of the vegetated compared to the nonvegetated sediment before meadow decline and showed  
470 no differences between sites during the decline, reflecting the higher organic matter content and  
471 corresponding demand for ABC transporters in seagrass-inhabited sediments [11, 15]. In addition,  
472 ABC transporters for sugars and amino acids showed an increase in their proportion in the bottom  
473 layer of the nonvegetated sediment from the period before decline to the period of meadow decline,  
474 which could be attributed to changes in organic matter content during the decline of the meadow.

475 The hydrolytic products of the degradation of complex organic matter, such as simple  
476 sugars and amino acids, can be imported and consumed by fermenting microbes. We have  
477 identified several enzymes involved in mediating various fermentation products, of which formate  
478 dehydrogenase, pyruvate:ferredoxin oxidoreductase, and alcohol dehydrogenase are the most  
479 abundant. Microcosm studies of the anaerobic degradation of organic matter in marine sediments  
480 revealed that acetate, formate, and ethanol are the most common fermentation products [102, 103].  
481 In addition, direct measurements of sediment pore water have revealed the presence of methanol  
482 and ethanol [104]. It is therefore not surprising that the most common fermentation-mediating  
483 enzymes we found are putatively involved in the metabolism of acetate, formate, and ethanol. In  
484 addition, pyruvate:ferredoxin oxidoreductase and alcohol dehydrogenase have also been reported  
485 to be important fermentation-mediating enzymes in Baltic Sea sediments [105]. Similar to the

486 dynamics of the ABC transporters, the fermentation-mediating enzymes also reflected the overall  
487 dynamics of the metabolic profile. Formate dehydrogenase, pyruvate:ferredoxin oxidoreductase,  
488 and alcohol dehydrogenase showed increased proportions in the deeper parts of the vegetated  
489 compared to the nonvegetated sediment before meadow decline, reflecting the higher organic matter  
490 content and possibly a higher fermentation rate in seagrass-inhabited sediments [11, 15].

491 The final step in the anaerobic degradation of organic matter involves the utilisation of simpler  
492 compounds such as SCFAs, including acetate and formate, and alcohols by the sulphate-reducing  
493 bacteria or methanogens [7, 9]. One of the most prominent proteins in functional COG category  
494 C was adenylylsulphate reductase, which is involved in dissimilatory sulphate reduction (Fig.  
495 6). Dissimilatory sulphate reduction is known to be a predominant terminal pathway of organic  
496 matter mineralisation in anoxic seabeds [90]. Sulphate adenylyltransferase (Sat), adenylylsulphate  
497 reductase (Apr), and dissimilatory sulphite reductase (Dsr), enzymes involved in the dissimilatory  
498 sulphate reduction pathway shared by known sulphate-reducing microorganisms [90], were also  
499 detected in our metaproteomic dataset. The dynamics of these enzymes showed some common  
500 patterns that were comparable to the overall dynamics of the metabolic profile. Overall, higher  
501 proportions of these enzymes were found in the deeper parts of the vegetated compared to the  
502 nonvegetated site before the meadow decline, while such differences were not present during decline.  
503 This pattern as well as the overall dynamics of the metabolic profile could be explained by the  
504 higher organic matter content in the seagrass-inhabited sediments before decline [11, 15] and by the  
505 increased input of fresh organic matter into the nonvegetated area during meadow decline, probably  
506 as a result of increased resuspension rates and sediment mixing [85].

507 Metaproteomics has great potential to provide insights into the microbial response to  
508 environmental change in marine systems [24]. In the present study, metaproteomic analysis of  
509 MS/MS spectra using sequenced metagenomes from a subset of the same samples led to the  
510 identification of 57,305 proteins, more than in other metaproteomic studies of marine sediments [26,  
511 28–30, 106]. Using this approach, it was possible to assess the dynamics of the metabolic profile

512 of microbial communities in the sediment of a declining *C. nodosa* meadow and the surrounding  
513 nonvegetated sediment. Consequently, it was possible to assess the impact of seagrass decline on  
514 the metabolic profile of these communities.

## 515 Conclusions

516 Seagrass sediments are considered natural hotspots for carbon sequestration, as some estimates  
517 suggest that up to 20 % of global carbon sequestration in marine sediments occurs in these  
518 carbon-rich sediments, although they occupy only 0.1 % of the seafloor [107–109]. Due to the  
519 role of seagrasses in carbon sequestration and their decline observed worldwide [31, 33–39], it is  
520 important to gain knowledge about the influence of this phenomenon on the processes carried out  
521 by the microbial community in the sediment.

522 The results of the present study show that the differences in the metabolic profile between the  
523 microbial communities inhabiting the vegetated and nonvegetated sediment, observed in the period  
524 before the meadow decline, disappeared during the decline. In addition, the metabolic profile of  
525 the nonvegetated communities approached that of the vegetated communities during the decline  
526 of the meadow. This phenomenon was more pronounced in the deeper parts of the nonvegetated  
527 sediment, indicating a stronger influence of the seagrass decline on the metabolic profile of the  
528 communities in this sediment layer. The differentiation between the vegetated and nonvegetated  
529 sediment when the meadow was present and the stronger shift in the profile observed in the deeper  
530 parts of the nonvegetated sediment during the decline could be explained by the intensity of the input  
531 of organic matter derived from the seagrass [11, 15]. The presence of the seagrass meadow reduces  
532 the intensity of resuspension, mixing, and transport between sites [85], thereby reducing the input  
533 of organic matter to the areas with bare sediment. However, with the decline of the seagrass, these  
534 processes are likely to be more intense, allowing organic matter to spread more easily throughout  
535 the area.

536 While these results provide a valuable foundation for future research, the relatively short  
537 sampling duration may not be sufficient to observe the full extent of microbial community response  
538 to seagrass decline, emphasising the need for longer-term studies. Furthermore, additional studies  
539 on microbial communities inhabiting sediments influenced by other seagrass species are needed to

540 confirm the generalisability of the results reported in this study.

## 541 **Declarations**

### 542 **Ethics approval and consent to participate**

543 Not applicable.

### 544 **Consent for publication**

545 Not applicable.

### 546 **Availability of data and material**

547 The raw metagenomic sequences obtained in this study have been deposited in the European  
548 Nucleotide Archive (ENA) at EMBL-EBI under the accession number PRJEB75905 (<https://www.ebi.ac.uk/ena/browser/view/PRJEB75905>). The mass spectrometry proteomics data have  
549 been deposited in the ProteomeXchange Consortium via the PRIDE [110] partner repository with  
550 the dataset identifier PXD054602. Following the recommendations given from the Riffomonas  
551 project to enhance data reproducibility (<http://www.riffomonas.org>), the detailed analysis procedure,  
552 including the R Markdown file for this article, is available as a GitHub repository ([https://github.com/MicrobesRovinj/Markovski\\_SalineSedimentMetap\\_EnvironMicrobiome\\_2025](https://github.com/MicrobesRovinj/Markovski_SalineSedimentMetap_EnvironMicrobiome_2025)).  
554

### 555 **Competing interests**

556 The authors declare that they have no competing interests.

557 **Funding**

558 This study was funded by the Croatian Science Foundation as part of the MICRO-SEAGRASS  
559 project (project number IP-2016-06-7118). GJH and ZZ were supported by the Austrian Science  
560 Fund (FWF; project number I 4978-B).

561 **Authors' contributions**

562 MN, GJH, and MK designed the study. MM, MN, ZZ, and MK performed sampling and  
563 laboratory analyses. MM, ZZ, and MK analysed the data. MM prepared the manuscript with  
564 editorial help from MN, ZZ, GJH, and MK. All authors reviewed the manuscript and approved the  
565 final submitted version.

566 **Acknowledgements**

567 We thank the Division of Computational Systems Biology (CUBE) of the University of Vienna  
568 for access to the Life Science Compute Cluster (LiSC) and Paolo Paliaga for his help with sampling.

569 **References**

- 570 1. Nealson KH. Sediment bacteria: Who's there, what are they doing, and what's new? *Annu Rev Earth Planet Sci.* 1997;25:403–34.
- 571 2. Hoshino T, Doi H, Uramoto G-I, Wörmer L, Adhikari RR, Xiao N, et al. Global diversity of  
573 microbial communities in marine sediment. *Proc Natl Acad Sci U S A.* 2020;117:27587–97.
- 574 3. Kallmeyer J, Pockalny R, Adhikari RR, Smith DC, D'Hondt S. Global distribution of microbial  
575 abundance and biomass in subseafloor sediment. *Proc Natl Acad Sci U S A.* 2012;109:16213–6.
- 576 4. Petro C, Starnawski P, Schramm A, Kjeldsen KU. Microbial community assembly in marine  
577 sediments. *Aquat Microb Ecol.* 2017;79:177–95.
- 578 5. Røy H, Kallmeyer J, Adhikari RR, Pockalny R, Jørgensen BB, D'Hondt S. Aerobic microbial  
579 respiration in 86-million-year-old deep-sea red clay. *Science.* 2012;336:922–5.
- 580 6. Jørgensen BB. Bacteria and marine biogeochemistry. In: Schulz HD, Zabel M, editors. *Marine  
581 geochemistry.* Berlin, Heidelberg: Springer; 2000. p. 169–206.
- 582 7. Arndt S, Jørgensen BB, LaRowe DE, Middelburg JJ, Pancost RD, Regnier P. Quantifying  
583 the degradation of organic matter in marine sediments: A review and synthesis. *Earth-Sci Rev.*  
584 2013;123:53–86.
- 585 8. Orsi WD. Ecology and evolution of seafloor and subseafloor microbial communities. *Nat Rev  
586 Microbiol.* 2018;16:671–83.
- 587 9. Suominen S, van Vliet DM, Sánchez-Andrea I, van der Meer MTJ, Sinninghe Damsté JS,  
588 Villanueva L. Organic matter type defines the composition of active microbial communities  
589 originating from anoxic Baltic Sea sediments. *Front Microbiol.* 2021;12:628301.
- 590 10. Arnosti C. Microbial extracellular enzymes and the marine carbon cycle. *Annu Rev Mar Sci.*  
591 2011;3:401–25.
- 592 11. Duarte CM, Holmer M, Marbà N. Plant–microbe interactions in seagrass meadows. In:  
593 Kristensenn E, Haese RR, Kostka JE, editors. *Interactions between macro- and microorganisms in  
594 marine sediments.* American Geophysical Union; 2005. p. 31–60.
- 595 12. Peduzzi P, Herndl GJ. Decomposition and significance of seagrass leaf litter (*Cymodocea*

- 596 *nodosa*) for the microbial food web in coastal waters (Gulf of Trieste, northern Adriatic Sea). Mar  
597 Ecol Prog Ser. 1991;71:163–74.
- 598 13. Liu S, Jiang Z, Deng Y, Wu Y, Zhao C, Zhang J, et al. Effects of seagrass leaf litter decomposition  
599 on sediment organic carbon composition and the key transformation processes. Sci China Earth Sci.  
600 2017;60:2108–17.
- 601 14. Trevathan-Tackett SM, Jeffries TC, Macreadie PI, Manojlovic B, Ralph P. Long-term  
602 decomposition captures key steps in microbial breakdown of seagrass litter. Sci Total Environ.  
603 2020;705:135806.
- 604 15. Mohapatra M, Manu S, Dash SP, Rastogi G. Seagrasses and local environment control the  
605 bacterial community structure and carbon substrate utilization in brackish sediments. J Environ  
606 Manage. 2022;314:115013.
- 607 16. Cúcio C, Engelen AH, Costa R, Muyzer G. Rhizosphere microbiomes of european seagrasses  
608 are selected by the plant, but are not species specific. Front Microbiol. 2016;7:440.
- 609 17. Zheng P, Wang C, Zhang X, Gong J. Community structure and abundance of archaea in a *Zostera*  
610 *marina* meadow: A comparison between seagrass-colonized and bare sediment sites. Archaea.  
611 2019;2019:5108012.
- 612 18. Alsaffar Z, Pearman JK, Cúrdia J, Ellis J, Calleja ML, Ruiz-Compean P, et al. The role  
613 of seagrass vegetation and local environmental conditions in shaping benthic bacterial and  
614 macroinvertebrate communities in a tropical coastal lagoon. Sci Rep. 2020;10:13550.
- 615 19. Sun Y, Song Z, Zhang H, Liu P, Hu X. Seagrass vegetation affect the vertical organization of  
616 microbial communities in sediment. Mar Environ Res. 2020;162:105174.
- 617 20. Zhang X, Zhao C, Yu S, Jiang Z, Liu S, Wu Y, et al. Rhizosphere microbial community  
618 structure is selected by habitat but not plant species in two tropical seagrass beds. Front Microbiol.  
619 2020;11:161.
- 620 21. Markovski M, Najdek M, Herndl GJ, Korlević M. Compositional stability of sediment microbial  
621 communities during a seagrass meadow decline. Front Mar Sci. 2022;9:966070.
- 622 22. Ettinger CL, Voerman SE, Lang JM, Stachowicz JJ, Eisen JA. Microbial communities in

- 623 sediment from *Zostera marina* patches, but not the *Z. marina* leaf or root microbiomes, vary in  
624 relation to distance from patch edge. PeerJ. 2017;5:e3246.
- 625 23. Wilmes P, Heintz-Buschart A, Bond PL. A decade of metaproteomics: Where we stand and  
626 what the future holds. Proteomics. 2015;15:3409–17.
- 627 24. Saito MA, Bertrand EM, Duffy ME, Gaylord DA, Held NA, Hervey WJ, et al. Progress and  
628 challenges in ocean metaproteomics and proposed best practices for data sharing. J Proteome Res.  
629 2019;18:1461–76.
- 630 25. Grossart H-P, Massana R, McMahon KD, Walsh DA. Linking metagenomics to aquatic microbial  
631 ecology and biogeochemical cycles. Limnol Oceanogr. 2020;65:S2–20.
- 632 26. Stokke R, Roalkvam I, Lanzen A, Haflidason H, Steen IH. Integrated metagenomic and  
633 metaproteomic analyses of an ANME-1-dominated community in marine cold seep sediments.  
634 Environ Microbiol. 2012;14:1333–46.
- 635 27. Glass JB, Yu H, Steele JA, Dawson KS, Sun S, Chourey K, et al. Geochemical, metagenomic  
636 and metaproteomic insights into trace metal utilization by methane-oxidizing microbial consortia in  
637 sulphidic marine sediments. Environ Microbiol. 2014;16:1592–611.
- 638 28. Urich T, Lanzén A, Stokke R, Pedersen RB, Bayer C, Thorseth IH, et al. Microbial community  
639 structure and functioning in marine sediments associated with diffuse hydrothermal venting assessed  
640 by integrated meta-omics. Environ Microbiol. 2014;16:2699–710.
- 641 29. Lin R, Lin X, Guo T, Wu L, Zhang W, Lin W. Metaproteomic analysis of bacterial communities  
642 in marine mudflat aquaculture sediment. World J Microbiol Biotechnol. 2015;31:1397–408.
- 643 30. Bargiela R, Herbst F-A, Martínez-Martínez M, Seifert J, Rojo D, Cappello S, et al.  
644 Metaproteomics and metabolomics analyses of chronically petroleum-polluted sites reveal  
645 the importance of general anaerobic processes uncoupled with degradation. Proteomics.  
646 2015;15:3508–20.
- 647 31. Dunic JC, Brown CJ, Connolly RM, Turschwell MP, Côté IM. Long-term declines and recovery  
648 of meadow area across the world's seagrass bioregions. Glob Change Biol. 2021;27:4096–109.
- 649 32. den Hartog C. The sea-grasses of the world. Amsterdam, London: North-Holland Publishing

- 650 Company; 1970.
- 651 33. Tuya F, Martín JA, Luque A. Impact of a marina construction on a seagrass bed at Lanzarote  
652 (Canary Islands). *J Coast Conserv.* 2002;8:157–62.
- 653 34. Orth RJ, Carruthers TJB, Dennison WC, Duarte CM, Fourqurean JW, Heck KL, et al. A global  
654 crisis for seagrass ecosystems. *BioScience.* 2006;56:987–96.
- 655 35. Tuya F, Ribeiro-Leite L, Arto-Cuesta N, Coca J, Haroun R, Espino F. Decadal changes in the  
656 structure of *Cymodocea nodosa* seagrass meadows: Natural vs. human influences. *Estuar Coast*  
657 *Shelf Sci.* 2014;137:41–9.
- 658 36. Fabbri F, Espino F, Herrera R, Moro L, Haroun R, Riera R, et al. Trends of the seagrass  
659 *Cymodocea nodosa* (Magnoliophyta) in the Canary Islands: Population changes in the last two  
660 decades. *Sci Mar.* 2015;79:7–13.
- 661 37. Orlando-Bonaca M, Francé J, Mavrič B, Grego M, Lipej L, Flander-Putrl V, et al. A new index  
662 (MediSkew) for the assessment of the *Cymodocea nodosa* (Ucria) Ascherson meadow's status. *Mar*  
663 *Environ Res.* 2015;110:132–41.
- 664 38. Orlando-Bonaca M, Francé J, Mavrič B, Lipej L. Impact of the port of Koper on *Cymodocea*  
665 *nodosa* meadow. *Ann Ser Hist Nat.* 2019;29:187–94.
- 666 39. Najdek M, Korlević M, Paliaga P, Markovski M, Ivančić I, Iveša L, et al. Dynamics of  
667 environmental conditions during the decline of a *Cymodocea nodosa* meadow. *Biogeosciences.*  
668 2020;17:3299–315.
- 669 40. Smith A, Kostka J, Devereux R, Yates D. Seasonal composition and activity of sulfate-reducing  
670 prokaryotic communities in seagrass bed sediments. *Aquat Microb Ecol.* 2004;37:183–95.
- 671 41. Guevara R, Ikenaga M, Dean AL, Pisani C, Boyer JN. Changes in sediment bacterial community  
672 in response to long-term nutrient enrichment in a subtropical seagrass-dominated estuary. *Microb*  
673 *Ecol.* 2014;68:427–40.
- 674 42. Bourque AS, Vega-Thurber R, Fourqurean JW. Microbial community structure and dynamics in  
675 restored subtropical seagrass sediments. *Aquat Microb Ecol.* 2015;74:43–57.
- 676 43. Pjevac P, Meier DV, Markert S, Hentschker C, Schweder T, Becher D, et al. Metaproteogenomic

- 677 profiling of microbial communities colonizing actively venting hydrothermal chimneys. *Front*  
678 *Microbiol.* 2018;9:680.
- 679 44. Zhou J, Bruns MA, Tiedje JM. DNA recovery from soils of diverse composition. *Appl Environ*  
680 *Microbiol.* 1996;62:316–22.
- 681 45. Li D, Liu C-M, Luo R, Sadakane K, Lam T-W. MEGAHIT: An ultra-fast single-node solution  
682 for large and complex metagenomics assembly via succinct de Bruijn graph. *Bioinformatics.*  
683 2015;31:1674–6.
- 684 46. Hyatt D, Chen G-L, LoCascio PF, Land ML, Larimer FW, Hauser LJ. Prodigal: Prokaryotic  
685 gene recognition and translation initiation site identification. *BMC Bioinformatics.* 2010;11:119.
- 686 47. Cantalapiedra CP, Hernández-Plaza A, Letunic I, Bork P, Huerta-Cepas J. eggNOG-mapper v2:  
687 Functional annotation, orthology assignments, and domain prediction at the metagenomic scale.  
688 *Mol Biol Evol.* 2021;38:5825–9.
- 689 48. Huerta-Cepas J, Szklarczyk D, Heller D, Hernández-Plaza A, Forslund SK, Cook H, et al.  
690 eggNOG 5.0: A hierarchical, functionally and phylogenetically annotated orthology resource based  
691 on 5090 organisms and 2502 viruses. *Nucleic Acids Res.* 2019;47:D309–14.
- 692 49. Buchfink B, Reuter K, Drost H-G. Sensitive protein alignments at tree-of-life scale using  
693 DIAMOND. *Nat Methods.* 2021;18:366–8.
- 694 50. Chourey K, Jansson J, VerBerkmoes N, Shah M, Chavarria KL, Tom LM, et al. Direct cellular  
695 lysis/protein extraction protocol for soil metaproteomics. *J Proteome Res.* 2010;9:6615–22.
- 696 51. Hultman J, Waldrop MP, Mackelprang R, David MM, McFarland J, Blazewicz SJ, et  
697 al. Multi-omics of permafrost, active layer and thermokarst bog soil microbiomes. *Nature.*  
698 2015;521:208–12.
- 699 52. Wiśniewski JR, Zougman A, Nagaraj N, Mann M. Universal sample preparation method for  
700 proteome analysis. *Nat Methods.* 2009;6:359–62.
- 701 53. Korlević M, Markovski M, Zhao Z, Herndl GJ, Najdek M. Selective DNA and protein isolation  
702 from marine macrophyte surfaces. *Front Microbiol.* 2021;12:665999.
- 703 54. Ryu S, Gallis B, Goo YA, Shaffer SA, Radulovic D, Goodlett DR. Comparison of a label-free

- 704 quantitative proteomic method based on peptide ion current area to the isotope coded affinity tag  
705 method. *Cancer Inform.* 2008;6:243–55.
- 706 55. Zhang Y, Wen Z, Washburn MP, Florens L. Improving label-free quantitative proteomics  
707 strategies by distributing shared peptides and stabilizing variance. *Anal Chem.* 2015;87:4749–56.
- 708 56. R Core Team. R: A language and environment for statistical computing. Vienna, Austria: R  
709 Foundation for Statistical Computing; 2025.
- 710 57. Wickham H, Averick M, Bryan J, Chang W, McGowan LD, François R, et al. Welcome to the  
711 tidyverse. *J Open Source Softw.* 2019;4:1686.
- 712 58. Wickham H. tidyverse: Easily install and load the tidyverse. 2023.
- 713 59. Xie Y. bookdown: Authoring books and technical documents with R Markdown. 2025.
- 714 60. Wilke CO. cowplot: Streamlined plot theme and plot annotations for ggplot2. 2024.
- 715 61. van den Brand T. ggh4x: Hacks for ggplot2. 2024.
- 716 62. FC M, Davis TL, ggplot2 authors. ggpattern: ggplot2 pattern geoms. 2025.
- 717 63. Ahlmann-Eltze C, Patil I. ggsignif: Significance brackets for ggplot2. 2022.
- 718 64. Zhu H. kableExtra: Construct complex table with kable and pipe syntax. 2024.
- 719 65. Xie Y. knitr: A general-purpose package for dynamic report generation in R. 2025.
- 720 66. Neuwirth E. RColorBrewer: ColorBrewer palettes. 2022.
- 721 67. Henry L, Wickham H. rlang: Functions for base types and core R and tidyverse features. 2025.
- 722 68. Allaire J, Xie Y, Dervieux C, McPherson J, Luraschi J, Ushey K, et al. rmarkdown: Dynamic  
723 documents for R. 2024.
- 724 69. Sherrill-Mix S. taxonomizr: Functions to work with NCBI accessions and taxonomy. 2025.
- 725 70. Xie Y. tinytex: Helper functions to install and maintain TeX Live, and compile LaTeX documents.  
726 2025.
- 727 71. Oksanen J, Simpson GL, Blanchet FG, Kindt R, Legendre P, Minchin PR, et al. vegan:  
728 Community ecology package. 2025.
- 729 72. Xie Y. bookdown: Authoring books and technical documents with R Markdown. Boca Raton,  
730 Florida: Chapman; Hall/CRC; 2016.

- 731 73. Constantin A-E, Patil I. *ggsignif*: R package for displaying significance brackets for 'ggplot2'.  
732 PsyArXiv. 2021. <https://doi.org/10.31234/osf.io/7awm6>.
- 733 74. Xie Y. *Dynamic documents with R and knitr*. 2nd edition. Boca Raton, Florida: Chapman;  
734 Hall/CRC; 2015.
- 735 75. Xie Y. *knitr: A comprehensive tool for reproducible research in R*. In: Stodden V, Leisch F,  
736 Peng RD, editors. *Implementing reproducible computational research*. Chapman; Hall/CRC; 2014.
- 737 76. Xie Y, Allaire JJ, Grolemund G. *R Markdown: The definitive guide*. Boca Raton, Florida:  
738 Chapman; Hall/CRC; 2018.
- 739 77. Xie Y, Dervieux C, Riederer E. *R Markdown cookbook*. Boca Raton, Florida: Chapman;  
740 Hall/CRC; 2020.
- 741 78. Xie Y. *TinyTeX: A lightweight, cross-platform, and easy-to-maintain LaTeX distribution based*  
742 *on TeX Live*. *TUGboat*. 2019;40:30–2.
- 743 79. Jost L. Entropy and diversity. *Oikos*. 2006;113:363–75.
- 744 80. Legendre P, Legendre L. *Numerical ecology*. 3rd edition. Amsterdam: Elsevier; 2012.
- 745 81. Borcard D, Gillet F, Legendre P. *Numerical ecology with R*. 2nd edition. Springer; 2018.
- 746 82. Duarte CM, Chiscano CL. Seagrass biomass and production: A reassessment. *Aquat Bot*.  
747 1999;65:159–74.
- 748 83. Duarte CM. Seagrass ecosystems. In: Levin SA, editor. *Encyclopedia of biodiversity*. 1st  
749 edition. Academic Press; 2001. p. 255–68.
- 750 84. Holmer M, Duarte CM, Boschker HTS, Barrón C. Carbon cycling and bacterial carbon sources  
751 in pristine and impacted Mediterranean seagrass sediments. *Aquat Microb Ecol*. 2004;36:227–37.
- 752 85. van Katwijk MM, Bos AR, Hermus DCR, Suykerbuyk W. Sediment modification by seagrass  
753 beds: Muddification and sandification induced by plant cover and environmental conditions. *Estuar*  
754 *Coast Shelf Sci*. 2010;89:175–81.
- 755 86. Habibi N, Uddin S, Al-Sarawi H, Aldhameer A, Shajan A, Zakir F, et al. Metagenomes from  
756 coastal sediments of Kuwait: Insights into the microbiome, metabolic functions and resistome.  
757 *Microorganisms*. 2023;11:531.

- 758 87. Kühlbrandt W. Structure and mechanisms of F-type ATP synthases. *Annu Rev Biochem.*  
759 2019;88:515–49.
- 760 88. Baykov AA, Malinen AM, Luoto HH, Lahti R. Pyrophosphate-fueled Na<sup>+</sup> and H<sup>+</sup> transport in  
761 prokaryotes. *Microbiol Mol Biol Rev.* 2013;77:267–76.
- 762 89. Luoto HH, Belogurov GA, Baykov AA, Lahti R, Malinen AM. Na<sup>+</sup>-translocating membrane  
763 pyrophosphatases are widespread in the microbial world and evolutionarily precede H<sup>+</sup>-translocating  
764 pyrophosphatases. *J Biol Chem.* 2011;286:21633–42.
- 765 90. Jørgensen BB, Findlay AJ, Pellerin A. The biogeochemical sulfur cycle of marine sediments.  
766 *Front Microbiol.* 2019;10:849.
- 767 91. Burdige DJ. Preservation of organic matter in marine sediments: Controls, mechanisms, and an  
768 imbalance in sediment organic carbon budgets? *Chem Rev.* 2007;107:467–85.
- 769 92. Aspeborg H, Coutinho PM, Wang Y, Brumer H, Henrissat B. Evolution, substrate specificity  
770 and subfamily classification of glycoside hydrolase family 5 (GH5). *BMC Evol Biol.* 2012;12:186.
- 771 93. Berlemont R, Martiny AC. Glycoside hydrolases across environmental microbial communities.  
772 *PLoS Comput Biol.* 2016;12:e1005300.
- 773 94. Drula E, Garron M-L, Dogan S, Lombard V, Henrissat B, Terrapon N. The carbohydrate-active  
774 enzyme database: Functions and literature. *Nucleic Acids Res.* 2022;50:D571–7.
- 775 95. Pfeifer L, Classen B. The cell wall of seagrasses: Fascinating, peculiar and a blank canvas for  
776 future research. *Front Plant Sci.* 2020;11:588754.
- 777 96. Torbatinejad N, Sabin J. Laboratory evaluation of some marine plants on South Australian  
778 beaches. *J Agric Sci Technol.* 2001;3:91–100.
- 779 97. Syed NNF, Zakaria MH, Bujang JS. Fiber characteristics and papermaking of seagrass using  
780 hand-beaten and blended pulp. *BioResources.* 2016;11:5358–80.
- 781 98. Zhou M-Y, Wang G-L, Li D, Zhao D-L, Qin Q-L, Chen X-L, et al. Diversity of both the  
782 cultivable protease-producing bacteria and bacterial extracellular proteases in the coastal sediments  
783 of King George Island, Antarctica. *PLoS One.* 2013;8:e79668.
- 784 99. Zhang X-Y, Han X-X, Chen X-L, Dang H-Y, Xie B-B, Qin Q-L, et al. Diversity of cultivable

- 785 protease-producing bacteria in sediments of Jiaozhou Bay, China. *Front Microbiol.* 2015;6:1021.
- 786 100. Liu Z, Liu G, Guo X, Li Y, Ji N, Xu X, et al. Diversity of the protease-producing bacteria  
787 and their extracellular protease in the coastal mudflat of Jiaozhou Bay, China: In response to clam  
788 naturally growing and aquaculture. *Front Microbiol.* 2023;14:1164937.
- 789 101. Wang S, Yan Z, Wang P, Zheng X, Fan J. Comparative metagenomics reveals the microbial  
790 diversity and metabolic potentials in the sediments and surrounding seawaters of Qinhuangdao  
791 mariculture area. *PLoS One.* 2020;15:e0234128.
- 792 102. Graue J, Engelen B, Cypionka H. Degradation of cyanobacterial biomass in anoxic tidal-flat  
793 sediments: A microcosm study of metabolic processes and community changes. *ISME J.*  
794 2012;6:660–9.
- 795 103. Pelikan C, Wasmund K, Glombitza C, Hausmann B, Herbold CW, Flieder M, et al. Anaerobic  
796 bacterial degradation of protein and lipid macromolecules in subarctic marine sediment. *ISME J.*  
797 2021;15:833–47.
- 798 104. Zhuang G-C, Lin Y-S, Elvert M, Heuer VB, Hinrichs K-U. Gas chromatographic analysis  
799 of methanol and ethanol in marine sediment pore waters: Validation and implementation of three  
800 pretreatment techniques. *Mar Chem.* 2014;160:82–90.
- 801 105. Zinke LA, Glombitza C, Bird JT, Røy H, Jørgensen BB, Lloyd KG, et al. Microbial organic  
802 matter degradation potential in Baltic Sea sediments is influenced by depositional conditions and in  
803 situ geochemistry. *Appl Environ Microbiol.* 2019;85:e02164–18.
- 804 106. Gillan DC, Roosa S, Kunath B, Billon G, Wattiez R. The long-term adaptation of bacterial  
805 communities in metal-contaminated sediments: A metaproteogenomic study. *Environ Microbiol.*  
806 2015;17:1991–2005.
- 807 107. Duarte CM, Kennedy H, Marbà N, Hendriks I. Assessing the capacity of seagrass meadows for  
808 carbon burial: Current limitations and future strategies. *Ocean Coastal Manage.* 2013;83:32–8.
- 809 108. Duarte CM, Middelburg JJ, Caraco N. Major role of marine vegetation on the oceanic carbon  
810 cycle. *Biogeosciences.* 2005;2:1–8.
- 811 109. Kennedy H, Beggins J, Duarte CM, Fourqurean JW, Holmer M, Marbà N, et al. Seagrass

812 sediments as a global carbon sink: Isotopic constraints. *Glob Biogeochem Cycles*. 2010;24:GB4026.

813 110. Perez-Riverol Y, Bai J, Bandla C, García-Seisdedos D, Hewapathirana S, Kamatchinathan

814 S, et al. The PRIDE database resources in 2022: A hub for mass spectrometry-based proteomics

815 evidences. *Nucleic Acids Res*. 2022;50:D543–52.